Environmental Microbiology (2000) **2**(4), 465–474

The responses of photosynthesis and oxygen consumption to short-term changes in temperature and irradiance in a cyanobacterial mat (Ebro Delta, Spain)

Eric Epping* and Michael Kühl†
Max-Planck-Institut für Marine Mikrobiologie, Microsensor Research Group, Celsiusstraße 1, D-28359, Bremen, Germany.

Summary

We have evaluated the effects of short-term changes in incident irradiance and temperature on oxygenic photosynthesis and oxygen consumption in a hypersaline cyanobacterial mat from the Ebro Delta, Spain, in which *Microcoleus chthonoplastes* was the dominant phototrophic organism. The mat was incubated in the laboratory at 15, 20, 25 and 30°C at incident irradiances ranging from 0 to 1000 μmol photons m^{-2} s^{-1}. Oxygen microsensors were used to measure steady-state oxygen profiles and the rates of gross photosynthesis, which allowed the calculation of areal gross photosynthesis, areal net oxygen production, and oxygen consumption in the aphotic layer of the mat. The lowest surface irradiance that resulted in detectable rates of gross photosynthesis increased with increasing temperature from 50 μmol photons m^{-2} s^{-1} at 15°C to 500 μmol photons m^{-2} s^{-1} at 30°C. These threshold irradiances were also apparent from the areal rates of net oxygen production and point to the shift of *M. chthonoplastes* from anoxygenic to oxygenic photosynthesis and stimulation of sulphide production and oxidation rates at elevated temperatures. The rate of net oxygen production per unit area of mat at maximum irradiance, J_0, did not change with temperature, whereas, J_{Zphot}, the flux of oxygen across the lower boundary of the euphotic zone increased linearly with temperature. The rate of oxygen consumption per volume of aphotic mat increased with temperature. This increase occurred in darkness, but was strongly enhanced at high irradiances, probably as a consequence of increased rates of photosynthate exudation, stimulating respiratory processes in the mat. The compensation irradiance (E_c) marking the change of the mat from a heterotrophic to an autotrophic community, increased exponentially in this range of temperatures.

Received 10 April, 2000; revised 29 May, 2000; accepted 1 June, 2000. †Present address: Marine Biological Laboratory, University of Copenhagen, Strandpromenaden 5, DK-3000 Helsingør, Denmark. *For correspondence and present address. Netherlands Institute for Sea Research, P.O.Box 59, 1790 AB den Burg, Texel, The Netherlands. E-mail epping@nioz.nl; Tel. (+31) 222 369440; Fax (+31) 222 319674.

Introduction

Benthic phototrophic microbial communities, developing in shallow and intertidal waters, may experience covarying temperature and irradiance oscillations on tidal, diurnal, seasonal and interannual time scales. The net growth of these communities results from the difference between the input of organic carbon due to oxygenic photosynthesis and the removal of organic carbon as a consequence of grazing, resuspension and subsequent export, and respiration. The responses of these processes to changes in temperature and light are important determinants for temporal variations in the productivity of these communities.

Numerous studies have considered temperature and irradiance as primary controlling factors of benthic net primary production on seasonal time scales (Pomeroy, 1959; Cadée and Hegeman, 1977; Rasmussen *et al*., 1983; Grant, 1986; Canfield and Des Marais, 1993; Pinckney and Zingmark, 1993). From these studies it has been inferred that seasonal changes in the photosynthetic response to incident light may be related to compositional changes (succession) and physiological adaptation of the community (Rasmussen *et al*., 1983; Grant, 1986; Hill and Boston, 1991; Guasch and Sabater, 1995). Relatively few studies have systematically considered the response of benthic phototrophic communities to changes in their thermal and photic environment on tidal and diurnal time scales (Pomeroy, 1959; Colijn and Van Buurt, 1975; Rasmussen *et al*., 1983; Grant, 1986). Short-term dynamics in benthic photosynthesis and respiration, however, can be expected to be as pronounced as the documented seasonal variations. Rasmussen *et al*. (1983) predicted a 24–90% increase in benthic photosynthesis due to the rise in temperature during low tide for temperate coastal sediments. In contrast, temperature changes mimicking emersion and immersion did not significantly alter the productivity of benthic phototrophic communities from intertidal sediments in Nova Scotia, Canada (Grant, 1986). These observations underscore the

potentially complex response of benthic oxygen metabolism to changes in temperature and incident irradiance.

In this study, the effects of short-term changes in temperature and irradiance on oxygenic photosynthesis and oxygen consumption in a hypersaline cyanobacterial mat are examined by the use of oxygen microsensors. A hypersaline mat was selected as a stratified model system, where bioturbating organisms are largely excluded and where negligible lateral variability in photosynthesis and oxygen consumption allows oxygen budgets to be calculated from oxygen microprofiles, after a simple, one-dimensional diffusion approach.

Results

Oxygen profiles

Average steady-state oxygen profiles ($n = 4–8$) for the experimental temperatures and irradiances are shown in Fig. 1. The thickness of the effective diffusive boundary layer, its upper boundary being defined as the height above the interface where the linear extrapolation of the gradient at the mat surface intercepts the bulk water oxygen concentration (Jørgensen and Revsbech, 1985), amounted to ~150 μm for all experimental conditions. This indicates that the hydrodynamic conditions and external control on the mat-water exchange processes were similar for all incubations.

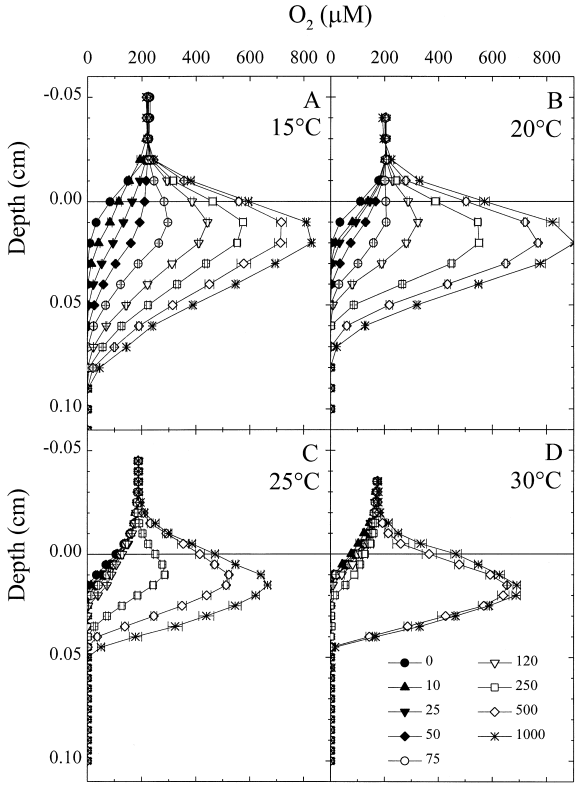

Fig. 1. Average steady-state oxygen profiles for a cyanobacterial mat incubated at (A) 15°C (B) 20°C (C) 25°C and (D) 30°C at various incident irradiances, as indicated by the numbers in the legend (unit: μmol photons m^{-2} s^{-1}). Error bars indicate ± 1 SD. ($n = 4–8$).

With increasing irradiance at 15°C (Fig. 1A), a subsurface maximum in oxygen concentration developed at 0.01–0.02 cm depth with oxygen penetrating to a maximum depth of 0.09 cm at 1000 μmol photons m^{-2} s^{-1}. At 20°C (Fig. 1B) the development of a subsurface maximum in oxygen concentration was less apparent at the lower irradiances as compared with the corresponding irradiances at 15°C. However, the subsurface oxygen maxima above 250 μmol photons m^{-2} s^{-1} were similar or higher to those recorded in the 15°C incubation. The maximum oxygen penetration depths, Z_{max}, at 20°C again increased with increasing surface irradiances, but were lower than the values for corresponding irradiances at 15°C. Raising the temperature to 25°C (Fig. 1C) and 30°C (Fig. 1D) revealed (i) a decrease in the subsurface maximum in oxygen concentration over the whole range of irradiances, (ii) a decreasing oxygen penetration depth to approximately 0.05 cm at 1000 μmol photons m^{-2} s^{-1}, and (iii) steeper downward gradients, being most pronounced at 500 and 1000 μmol photons m^{-2} s^{-1}.

Gross photosynthesis

Figure 2 compiles the average rates of gross photosynthesis ($n = 3–8$) against depth in the mat for the experimental combinations of temperature and irradiance. In general, gross photosynthetic activities were moderate at the mat surface, showed a maximum at 0.01 cm depth, and then decreased with depth. The maximum thickness of the euphotic zone was observed at maximum irradiance and amounted to 0.04 cm at 20°C and 0.03 cm for the other temperatures. From these measurements a threshold irradiance for gross photosynthesis was observed, i.e. a minimum surface irradiance was required for detectable rates of gross photosynthesis. This threshold irradiance increased with increasing incubation temperatures from 50 μmol photons m^{-2} s^{-1} at 15°C to 500 μmol photons m^{-2} s^{-1} at 30°C.

During overnight preincubations at 25°C and 30°C, *Beggiatoa* sp. migrated towards the mat–water interface. These gliding sulphur oxidizing bacteria resided at the mat–water interface at irradiances below the threshold value, but migrated downward at the threshold irradiance, indicating that the sulphide–oxygen boundary moved downward as a consequence of oxygenic photosynthesis.

Oxygen budget calculations

The effects of temperature and irradiance on gross photosynthesis were evaluated from the areal rates of

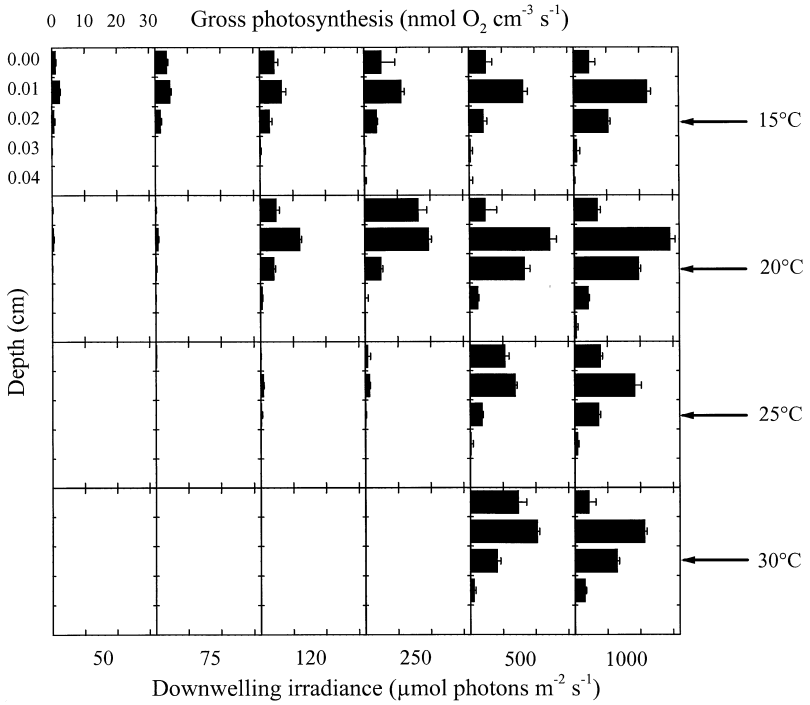

Fig. 2. Average rates of oxygenic gross photosynthesis ($n = 3–8$) against depth in a cyanobacterial mat incubated at 15°C, 20°C, 25°C and 30°C. Photosynthetic rates at irradiances below 50 μmol photons m^{-2} s^{-1} are not shown.

gross photosynthesis rather than from the activity at a specific depth interval in order to minimize the effect of vertical migration on this analysis. The areal rates of gross photosynthesis were calculated (see eqn 3) from Fig. 2 and are plotted against the surface downwelling irradiance for the different experimental temperatures in Fig. 3. These areal rates confirm the threshold irradiance for oxygenic photosynthesis, increasing from 50 μmol photons m^{-2} s^{-1} at 15°C to 500 μmol photons m^{-2} s^{-1} at 30°C. From these data, it can be inferred that at low irradiances and higher temperatures, light was not used for oxygenic photosynthesis. Although the areal rates of gross photosynthesis at 15°C (Fig. 3A) and 20°C (Fig. 3B) display a quasi-saturation behaviour with increasing incident irradiances, full saturation was not observed because gross photosynthesis in 'deeper' layers was still increasing at the maximum applied level of irradiance (cf. Fig. 2). At 25°C (Fig. 3C) and 30°C (Fig. 3D) the areal rates of gross photosynthesis did show saturation at ≈500 μmol photons m^{-2} s^{-1}. The areal rates of gross photosynthesis at 1000 μmol photons m^{-2} s^{-1} are plotted against the experimental temperature in Fig. 4.

Mat-water fluxes of oxygen, J_0, were calculated (eqn 1) from the steady-state oxygen profiles in Fig. 1 and plotted as a function of the downwelling irradiance at different temperatures in Fig. 3. J_0 showed threshold irradiances at similar values as gross photosynthesis. Above the threshold irradiance, J_0 decreased exponentially with increasing irradiance to an asymptotic value at all temperatures. The

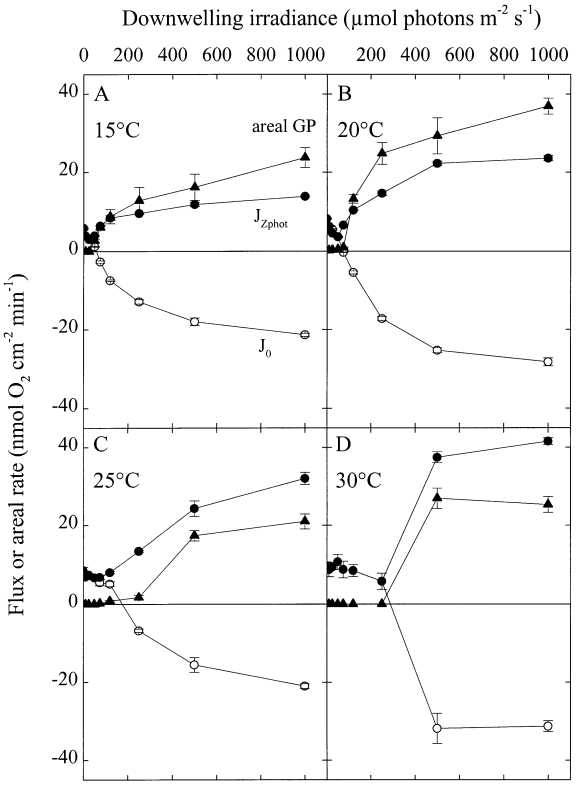

Fig. 3. Steady-state fluxes of oxygen across the mat–water interface (J_0), across the lower boundary of the euphotic layer (J_{Zphot}), and areal gross photosynthesis (areal GP) as a function of incident irradiance for the experimental temperatures. Fluxes were calculated from the oxygen profiles in Fig. 1. Positive values indicate downward oxygen fluxes.

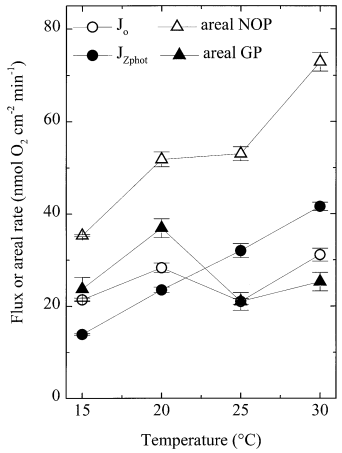

Fig. 4. Steady-state fluxes of oxygen across the mat–water interface (J_0), across the lower boundary of the photic layer (J_{Zphot}), areal net oxygen production in the euphotic zone (areal NOP), and areal gross photosynthesis (areal GP) at 1000 μmol photons m^{-2} s^{-1} as a function of incubation temperature.

(absolute) asymptotic value, however, did not show a clear trend with temperature as depicted in Fig. 4.

In order to calculate the oxygen flux across the lower boundary of the of the photic layer, Z_{phot} was deduced from the photosynthesis profiles in Fig. 2. For irradiances that did not result in detectable rates of gross photosynthesis, the thickness of the euphotic layer was assumed to equal 0 and, consequently, the calculated fluxes at Z_{phot} are identical to J_0 (Fig. 3). J_{Zphot} showed threshold irradiances, similar to gross photosynthesis and the mat-water fluxes. At irradiances above the threshold value J_{Zphot} increased concomitantly with the development of subsurface maxima in oxygen concentration. The downward fluxes at the lower boundary of the euphotic layer saturated at the highest experimental light intensities. The saturation values of downward fluxes, plotted in Fig. 4, increased with increasing temperatures from ≈ 14 nmol O_2 cm^{-2} min^{-1} at 15°C up to 42 nmol O_2 cm^{-2} min^{-1} at 30°C.

The rates of areal net oxygen production for the euphotic layer, calculated by summing the fluxes across the sediment–water interface and Z_{phot} (eqn 5, data not shown), confirmed the threshold irradiances for oxygenic photosynthesis. The values for areal net oxygen production in the euphotic layer at maximum irradiance increased from approximately 40 nmol O_2 cm^{-2} min^{-1} at 15°C up to 75 nmol O_2 cm^{-2} min^{-1} at 30°C and are presented in Fig. 4 as well.

Figure 4 summarizes the fluxes and productivities at 1000 μmol photons m^{-2} s^{-1}. A similar trend was observed for areal rates of gross photosynthesis and the mat-water fluxes on the one hand and for areal net oxygen production in the euphotic layer and downward fluxes across the euphotic boundary on the other hand. Areal gross photosynthesis and mat-water fluxes showed no increase with increasing temperature, whereas downward fluxes and areal net oxygen production did. Apparently, the increase in areal net oxygen production in the euphotic layer resulted from stronger downward fluxes with increasing temperatures. Increased downward fluxes indicate enhanced rates of oxygen consumption in the aphotic oxic mat as temperature increased.

This effect of temperature on the rate of oxygen consumption was evaluated for darkness and for the aphotic layer at 500 and 1000 μmol photons m^{-2} s^{-1}, the only two irradiances that resulted in gross photosynthesis at all temperatures. The rates of oxygen consumption were assessed from the oxygen profiles in Fig. 1, using eqns 2 and 7 respectively. In the dark, the rate of oxygen consumption increased with temperature from 196 nmol O_2 cm^{-3} min^{-1} at 15°C to 630 nmol O_2 cm^{-3} min^{-1} at 30°C (Fig. 5A), corresponding to an apparent activation energy or temperature characteristic (Abdollahi and Nedwell, 1979) of 55 kJ mol^{-1} (Fig. 5B) and a temperature coefficient, Q_{10}, of 2.35.

At 500 μmol photons m^{-2} s^{-1} the rate of oxygen consumption increased from 235 nmol O_2 cm^{-3} min^{-1} at 15°C to 3740 nmol O_2 cm^{-3} min^{-1} at 30°C, whereas at 1000 μmol photons m^{-2} s^{-1} these rates were 280 and 4150 nmol O_2 cm^{-3} min^{-1} respectively (Fig. 5A). The temperature characteristics for oxygen consumption at these light intensities were very similar: 134 kJ mol^{-1} at 500 μmol photons m^{-2} s^{-1} and 136 kJ mol^{-1} at 1000 μmol photons m^{-2} s^{-1}, yielding temperature coefficients of 6.6 and 6.7 respectively.

Both the rate of oxygen consumption as well as the threshold irradiances for gross photosynthesis increased with increasing temperature. Consequently, the irradiance at which the mat changes from a net oxygen consuming community into a net oxygen producing community, the compensation irradiance E_c, should increase with increasing temperature. The compensation irradiance increased exponentially from ≈ 55 μmol photons m^{-2} s^{-1} at 15°C to 290 μmol photons m^{-2} s^{-1} at 30°C (Fig. 6).

Both the areal rate of gross photosynthesis and the areal rate of net oxygen production in the euphotic layer displayed a threshold irradiance at similar values, which increased with increasing incubation temperature (Fig. 3). However, the data in Figs 3 and 4 clearly demonstrate that areal gross photosynthesis is too low to sustain areal net oxygen production in the euphotic layer at all experimental temperatures. In Fig. 7, the areal rates of gross photosynthesis are plotted against the areal rates of net oxygen production in the euphotic layer for the experimental temperatures. The straight line indicates unity for these quantities, which should be obtained in the absence of oxygen consumption in the euphotic layer (i.e. all oxygen which is produced by oxygenic photosynthesis diffuses across the upper or lower boundary of the

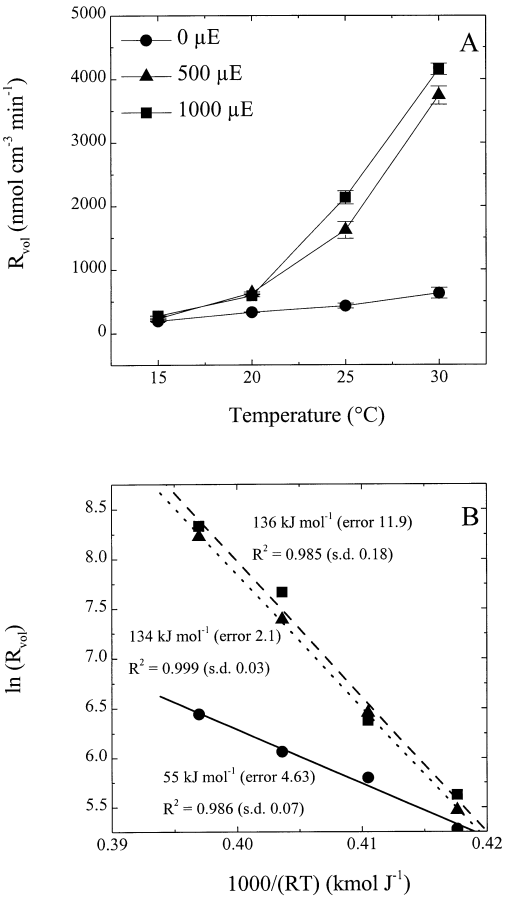

Fig. 5. A. Rates of oxygen consumption per volume of mat, R_{vol}, during darkness and in the aphotic oxic layer at 500 and 1000 μmol photons m^{-2} s^{-1} plotted against the experimental incubation temperatures.
B. Arrhenius plot representation of the oxygen consumption rates as shown in panel (A). Lines represent the linear regressions to yield the temperature characteristics as indicated in the plot.

euphotic zone). The discrepancy between the quantities appears most severe at 25°C and 30°C and areal rates of gross photosynthesis may have been underestimated by at least up to a factor of 2.5 at 30°C at an incident irradiance of 1000 μmol photons m^{-2} s^{-1}. As a consequence of this underestimation, the rates of oxygen consumption in the euphotic layer could not be deduced from the comparison of areal gross and areal net oxygen production.

Discussion

The initial slope of the photosynthesis ~ irradiance curve is generally considered to be independent of temperature (e.g. Jassby and Platt, 1976), although recent studies have shown a reduction in the initial slope with increasing incubation temperature (Davison, 1991). In contrast, the specific rate of photosynthesis under light saturating conditions is strongly dependent on temperature (Blanchard *et al.*, 1996) as it is mainly determined by the activities of the enzymes involved in carbon dioxide fixation (Li *et al.*, 1984; Sukenik *et al.*, 1987; Rivkin, 1990). Neither characteristic was observed for the mat from the Ebro Delta: the threshold irradiance for both gross photosynthesis and net oxygen production increased with increasing temperature, whereas the maximum areal rate of gross photosynthesis appeared invariant with temperature. The threshold irradiance may be attributed to the apparent underestimation of gross photosynthesis, to the metabolic versatility of *Microcoleus chthonoplastes,* or a shading effect of *Beggiatoa* sp. These options will be discussed below.

Gross photosynthesis measurements

The disparity between areal rates of gross photosynthesis and areal net oxygen production in the euphotic layer may be due to an underestimation of gross photosynthesis, to an overestimation of areal net oxygen production, or to both. Obviously, the chosen values for mat porosity and mat diffusion coefficient in order to estimate diffusivity ($\phi \times D_s$) represent a potential source of error in the flux calculations. Diffusivity estimations for a biologically active, temperate cyanobacterial mat at 20°C, using nitrous oxide as a tracer, ranged from 1.15×10^{-5} to 1.74×10^{-5} cm^2 s^{-1} with an average value of 1.41×10^{-5} cm^2 s^{-1} (Glud *et al.*, 1995). For comparison, our assumptions for porosity and for *n* resulted in a diffusivity of 1.58×10^{-5} cm^2 s^{-1} at this temperature, which is at the higher end of the reported range. For all experimental temperatures, the estimated diffusivities may have resulted in some overestimation of downward

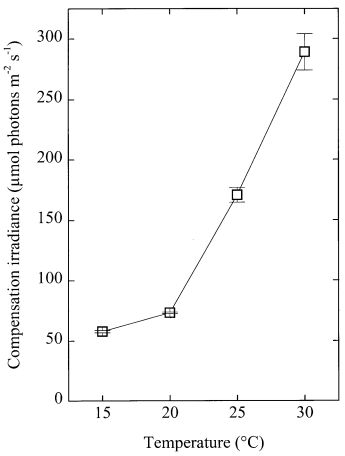

Fig. 6. Compensation irradiances (E_c) for the mat as a function of the incubation temperature. E_c values were estimated from the steady-state fluxes of oxygen across the mat–water interface shown in Fig. 3.

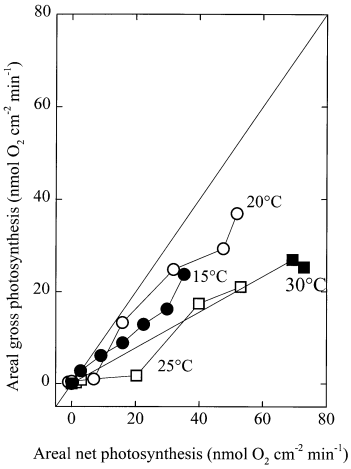

Fig. 7. Areal rates of gross photosynthesis plotted against the calculated rates of areal net oxygen production in the euphotic layer for different experimental incubation temperatures. The straight line indicates unity, i.e. no oxygen is consumed in the euphotic layer.

fluxes and consequently of areal net oxygen production in the euphotic layer. However, a reduction of downward fluxes in order to match the areal rates of net and gross photosynthesis would require extremely low diffusivities ($\phi \times D_s < 10\%$ of the free solution molecular diffusion coefficient). Moreover, for several experimental conditions the areal rates of gross photosynthesis cannot sustain the oxygen fluxes from the mat towards the overlying water, which were calculated from a well-defined free solution diffusion coefficient without the need for tortuosity and porosity correction. The disparity between the areal rates of net and gross photosynthesis should thus be attributed to underestimated rates of gross photosynthesis rather than to an overestimation of diffusivity within the mat.

Because all methodological criteria for the application of the microsensor light–dark shift method were met, i.e. fast responding electrodes and measuring circuits, high time resolution of data acquisition, and short dark periods, we can only speculate on the cause for this underestimation. In a recent paper, Pamatmat (1997) pointed to the role of hydrogen peroxide as a source of non-photosynthetic O_2 production in the dark. Microbial mats might be excellent sites for intensive hydrogen peroxide cycling (M. Kühl, unpublished data), both in the light and in darkness (for an overview of the reactions see Pamatmat, 1997). The alleviation of light inhibition on catalase upon darkening during the light–dark shift procedure may have resulted in a faster decomposition of hydrogen peroxide to oxygen, resulting in a lesser initial decrease in oxygen concentration and consequently in an underestimation of gross photosynthesis. Although the process rates and concentrations are considerably different in microbial mats compared with open waters, the mechanism and the ultimate effect on the estimates of gross photosynthesis may be quite similar and merits further attention for microbial mats. This underestimation of gross photosynthesis neither affects the calculation of mat–water fluxes and net oxygen production nor oxygen consumption activities in the zone underlying the euphotic layer. It will, however, to an unknown extent influence the gross photosynthesis compared with the irradiance relations as shown in Fig. 3 and compared with temperature in Fig. 4.

The threshold irradiances were evident not only for gross photosynthesis, but also for the areal rates of net oxygen production in the mat and the euphotic layer. Because these quantities are determined by independent methods, the threshold is not to be considered as an artifact of the gross photosynthesis measurements. The threshold for oxygenic photosynthesis and its increase with increasing temperature can presumably be explained by temperature induced changes in the metabolism of *M. chthonoplastes*.

Metabolic versatility of M. chthonoplastes

The observed migration of *Beggiatoa* sp. supports the concept that *M. chthonoplastes* switched from an alternative metabolism to oxygenic photosynthesis at the threshold irradiances. At 25°C and 30°C, the chemolithotrophic sulphide oxidizing bacterium *Beggiatoa* sp. resided at the mat–water interface at incident irradiances below the threshold value, indicating that the oxygen–sulphide boundary was close to the mat–water interface up to this irradiance (Nelson *et al*., 1986). The population of *M. chthonoplastes* underneath would consequently have been exposed to hydrogen sulphide, which has been shown to be an inhibitor of photosystem II and to be a suitable electron donor for anoxygenic photosynthesis (Castenholz, 1976; Garlick *et al*., 1977; Cohen *et al*., 1986; Jørgensen *et al*., 1986). *M. chthonoplastes* is metabolically a highly versatile microorganism and appears well adapted to short periods of anoxia and high-sulphide concentrations (Cohen *et al*., 1986; De Wit *et al*., 1988). The capability of simultaneous operation of oxygenic and anoxygenic photosynthesis allows an efficient transition between these modes of photoautotrophic metabolism (Cohen *et al*., 1986; Jørgensen *et al*., 1986; De Wit *et al*., 1988). It is, however, an aerobic organism because it does not possess a completely anaerobic metabolism and requires oxygen as a micronutrient for the synthesis of poly unsaturated fatty acids (Padan, 1979) and growth (De Wit *et al*., 1988). Short-term incubations of photoautotrophically grown cells under anaerobic conditions, however, have demonstrated that this cyanobacterium is capable of fermenting glycogen independent of *de novo* protein synthesis (Moezelaar and Stal, 1994). In a dynamic and steep-gradient ecosystem such as a

cyanobacterial mat, the population of *M. chthonoplastes* encounters conditions, temporarily and spatially, that may invoke all these different modes of metabolism.

Our experiments suggest that *M. chthonoplastes* changed from anoxygenic photosynthesis at irradiances below the threshold value to oxygenic photosynthesis at higher irradiances. We speculate that the increase in temperature resulted in increasing rates of sulphate reduction (Vosjan, 1974; Abdollahi and Nedwell, 1979), which raised the concentration of hydrogen sulphide within the mat as recently demonstrated by Wieland and Kühl (2000). Elevated sulphide concentrations would enhance the diffusive transport of sulphide towards the mat–water interface resulting in an upward shift of the oxygen–sulphide boundary as indicated by the upward migration of *Beggiatoa* sp. At irradiances below the threshold value, hydrogen sulphide would suppress oxygenic photosynthesis and would prevent the evolution of oxygen in the photic zone. Because increasing irradiances alleviated this sulphide inhibition, the removal of sulphide should be a light dependent reaction. Therefore, it is suggested that at least some fraction of the *M. chthonoplastes* population performed anoxygenic photosynthesis at irradiances below the threshold value in line with earlier observations of *M. chthonoplastes* photosynthesis in cyanobacterial mats (Cohen *et al*., 1986). With increasing surface irradiances and increased rates of anoxygenic photosynthesis, the uppermost layer of the mat would gradually be depleted in sulphide by the combined activities of chemolithotrophic sulphide oxidation and anoxygenic photosynthesis, resulting in the re-establishment of oxygenic photosynthesis and downward migration of *Beggiatoa* sp.

Another effect of the presence of *Beggiatoa* sp. at the mat surface at elevated temperatures and low irradiance could be a shading of the underlaying cyanobacteria, which could also cause an increase in the threshold irradiance. However, we did not apply microscale irradiance measurements (Kühl *et al*., 1997) in this study, and the extent of shading due to *Beggiatoa* remains to be shown.

The effect of temperature on oxygen consumption

The temperature coefficient for oxygen consumption in the dark corresponds well with the reported values for microbiological processes in the literature (Vosjan, 1974; Abdollahi and Nedwell, 1979; Thamdrup *et al*., 1998). At saturating incident irradiances, however, the temperature coefficient for oxygen consumption in the aphotic layer was much higher. This suggests that oxygen consumption at saturating incident irradiances was enhanced by additional factors than merely the increase in temperature. During photosynthesis, a diverse suite of organic compounds is produced and partially released into the environment. A number of studies has shown that these compounds can readily be assimilated and recycled by associated heterotrophic bacteria (Bauld and Brock, 1974; Bateson and Ward, 1988; Epping *et al*., 1999). Bateson and Ward (1988) have shown that 80% of this extracellular release may consist of glycolate, the product of photorespiration. Photorespiration due to the oxygenase activity of RuBisco is believed to increase with temperature because the affinity constant of RuBisco for O_2 increases more slowly with temperature than for CO_2 (Berry and Raison, 1981). The exposure of the mat to high irradiances and temperatures, resulting in high oxygen concentrations, could have promoted the release of glycolate and may have stimulated the rate of oxygen consumption in the aphotic layer. It has previously been postulated that the release of photosynthate may stimulate daytime sulphate reduction (Fründ and Cohen, 1992; Canfield and Des Marais, 1993). Therefore, the increase in oxygen consumption, as observed in our study, may not only have resulted from an increase in heterotrophic oxygen respiration (Kühl *et al*., 1996; Epping *et al*., 1999) but from enhanced sulphide oxidation rates as well.

The compensation irradiance and its ecological implication

The increase in threshold irradiance for oxygenic photosynthesis could indicate that the relative contribution of anoxygenic photosynthesis to the total of carbon fixation by *M. chthonoplastes* increased with rising temperatures. Because *M. chthonoplastes* is the dominant oxygenic phototrophic organism in this cyanobacterial mat, its metabolic shift from anoxygenic to oxygenic photosynthesis is clearly reflected in the compensation irradiance for the mat, as deduced from the oxygen fluxes across the mat–water interface. The compensation irradiance roughly marks the transition of the mat from a heterotrophic to an autotrophic state. This even applies to the case of extensive anoxygenic photosynthesis, as the sulphide that is oxidized through anoxygenic photosynthesis is not oxidized by oxygen and consequently does not add to the mineralization term of the mat. However, anoxygenic photosynthesis does not add to a net increase in mat biomass either, despite the fact that it is a primary production pathway by definition. It should be considered as regenerative production, because it recycles the hydrogen sulphide and inorganic carbon produced during carbon mineralization with sulphate as the terminal electron acceptor. The net effect of coupled sulphate reduction and anoxygenic photosynthesis on the pool size of organic carbon is ultimately determined by the relative growth yields of sulphate reducing bacteria and anoxygenic phototrophic organisms. Although small

differences in growth yield may become significant at high turnover rates of the substrates, the net effect of these coupled pathways on the organic carbon budget for the mat is probably negligible compared with that of oxygenic photosynthesis and oxygen consumption in this mat. Therefore, the oxygen flux across the mat–water interface is probably a good predictor for the balance of inorganic carbon fixation and organic carbon oxidation, although an exact balance requires corrections for the molar growth yields and the loss of reducing equivalents, such as the burial of sulphides and diffusion of hydrogen sulphide into the overlying water at high temperatures and dim light.

Obviously, the quantitative significance of metabolic shifts invoked by changes in temperature and irradiance on the estimate of a daily carbon budget as observed for this mat is determined by the *in situ* diurnal cycles of temperature and irradiance.

Experimental procedures

Cyanobacterial mats

Mats were collected from the salterns at Alfacs Peninsula in the Ebro Delta, Spain, in November 1995. The sampling area has a coastal Mediterranean climate with temperatures ranging from 3 to >27°C (Mir *et al*., 1991) and maximum solar irradiances of 2200 μmol photons m^{-2} s^{-1} during summer (Guerrero *et al*., 1993). At the time of sampling, the salinity of the overlying water was 55‰ and the water temperature was 20°C. Intact pieces of mat (~100 cm^2) were stored in plastic bags under moist atmosphere and transported to the laboratory. Macroscopically, the mat showed a simple lamination of a ± 1 mm thick, dark green, coherent surface layer on top of a reduced, black layer with a high content of lithogenic material. *M. chthonoplastes* was tentatively identified as the dominant mat-forming filamentous cyanobacterium (F. Garcia-Pichel, personal communication). Scattered throughout the surface layer coccoid, uni-cellular cyanobacteria were present in low abundance, whereas diatoms were virtually absent. A discrete pink layer, indicating a high abundance of purple sulphur bacteria, could not be observed. Instead, *Beggiatoa* sp., a microaerophilic chemolithotrophic sulphide oxidizing bacterium, formed a dense white cover at the mat–water interface during incubations at high temperatures in combination with low incident irradiances.

Subsamples of the mat (4×5 cm) were immobilized in a flow chamber (Lorenzen *et al*., 1995) by a 2% (w/v) agar solution, leaving the mat surface freely exposed to the overlying water. Artificial sea water (HW Meersalz) was circulated through the chamber to create a smooth turbulent flow over the mat. To mimic natural conditions, the water was essentially free of inorganic nutrients, and had a salinity of 55‰ at pH 8. The reservoir water (6 l volume) was aerated and temperature controlled ($\pm$ 0.5°C; Lauda RC6). The mat surface was illuminated by a collimated light beam at an incident angle of 60° using a 150 W fibre-optic tungsten-halogen light source (Schott KL 1500). Incident irradiance at the mat surface was altered by inserting neutral density filters (Oriel) in the light path. The downwelling scalar irradiance was measured by replacing the flow chamber by a 400–700 nm quantum scalar irradiance sensor (Biospherical Instruments QSL-100) placed over a light trap.

The experimental work started with a preincubation of the mat overnight in darkness at 15°C. The following morning, 4–8 replicate oxygen profiles were measured under dark conditions. Subsequently, the downwelling irradiance was set to 10 μmol photons m^{-2} s^{-1}. After incubation for ≈ 1 h, steady-state oxygen profiles ($n = 4$–8) and the vertical distribution of gross oxygenic photosynthesis were measured (3–8 replicate measurements for each depth). This procedure was followed for steady-state conditions at 25, 50, 75, 120, 250, 500 and 1000 μmol photons m^{-2} s^{-1}. After completing the measurements for all irradiances at 15°C, the temperature was increased to 20°C and the mat was again preincubated overnight in darkness. The procedure for measuring oxygen profiles and oxygenic photosynthesis at 20, 25 and 30°C was identical to the incubation at 15°C, resulting in a total of 32 combinations of temperature and downwelling irradiance. The transition times between steady states, as judged from the reproducibility of subsequent oxygen microprofiles, were less than 1 h at 15 or 20°C, but increased to over 1.5 h at 30°C.

Oxygen and gross photosynthesis measurements

The concentration of dissolved oxygen and the rates of gross photosynthesis were measured with Clark-type oxygen microsensors as outlined in Epping *et al*. (1999), based on the principles and methodology originally described in Revsbech (1989) and Revsbech and Jørgensen (1983).

Calculations

Oxygen budgets were calculated for all experimental conditions by quantifying the sink and source terms for oxygen per unit area of mat surface per unit time. In the following, the sink terms will not be differentiated and are collectively referred to as 'oxygen consumption'. The flux of oxygen across the mat–water interface (J_o) was calculated from Fick's first law of diffusion:

$$J_0 = -D_0 \frac{dC}{dz} \quad (1)$$

where C is the oxygen concentration, z is the depth coordinate (zero at the mat–water interface, scaled positively downward). D_0 is the free solution molecular diffusion coefficient for oxygen, corrected for temperature and salinity (Broecker and Peng, 1974; Li and Gregory, 1974). At a salinity of 55‰ and a temperature of 20°C, D_0 amounts to 1.91×10^{-5} cm^2 s^{-1}. dC/dz was determined from the linear section of the concentration gradient in the diffusive boundary layer (DBL), where molecular diffusion strongly dominates the mass transfer of oxygen. The average rate of oxygen consumption per volume of wet mat, R_{vol}, can be calculated from the areal rate of oxygen consumption and the maximum penetration depth of oxygen, Z_{max}:

$$R_{vol} = \frac{J_0}{Z_{max}} \quad (2)$$

When exposed to light, the mat receives additional oxygen from benthic oxygenic photosynthesis. As the measured rates of gross photosynthesis represent activities per volume of pore water, these should be corrected for mat porosity, ϕ, to calculate gross photosynthesis per volume of wet mat or per unit area of mat. Because a substantial part of the mat consists of intact cells with intracellular water it is difficult to estimate porosity by standard drying procedures (Canfield and Des Marais, 1993; Glud *et al*., 1995). Therefore, we have assumed a depth independent porosity of 0.95 and calculated areal gross photosynthesis, P_{area}, from:

$$P_{\text{area}} = \phi \Delta z \sum_{z=0}^{z=Zphot} P(z) \tag{3}$$

where Δz is the depth interval for the measurement, i.e. 0.01 cm, and Z_{phot} is the depth of the euphotic zone. In practice, this depth corresponded to the deepest interval in which gross photosynthesis could be detected by the procedure as described above. Thus, the general steady-state oxygen mass balance per unit area of mat for both dark and light conditions is given by:

$$P_{\text{area}} + J_0 = R_{\text{area}} \tag{4}$$

Note that the sign of J_0 is positive in case of a flux directed towards the mat and negative when directed towards the overlying water.

The rate of areal net oxygen production for the euphotic layer with lower boundary at Z_{phot} is defined as the difference between gross photosynthesis and oxygen consumption in this layer. In steady state, areal net oxygen production is equal to the export of oxygen from the euphotic layer across the upper and lower boundary:

$$net\mathrm{P}_{areal}^{phot} = J_{Zphot} - J_0 \tag{5}$$

J_{Zphot}, the oxygen flux at the lower boundary, is again calculated from Fick's first law of diffusion:

$$J_{Zphot} = -\phi D_{\text{s}} \left.\frac{dC}{dz}\right|_{Zphot} \tag{6}$$

where $dC/dz|_{Zphot}$ represents the concentration gradient of oxygen at Z_{phot} and D_{s} is the tortuosity corrected molecular diffusion coefficient for oxygen, calculated from:

$$D_s = \frac{D_0}{1 + n(1 - \phi),}$$

(Iversen and Jørgensen, 1993).

For $n = 3$ and $\phi = 0.95$, the values for diffusivity ($\phi \times D_s$) are 1.37×10^{-5}, 1.58×10^{-5}, 1.79×10^{-5}, and 2.02×10^{-5} cm^2 s^{-1} at 15, 20, 25, and 30°C respectively.

Similar to eqn 2, the average rate of oxygen consumption in the aphotic oxic layer per volume of wet mat can be calculated from the downward flux at Z_{phot} and the thickness of the aphotic oxic layer from:

$$R_{vol}^{aphot} = \frac{J_{Zphot}}{Z_{\text{max}} - Z_{phot}} \tag{7}$$

Acknowledgements

The authors wish to thank Gaby Eickert and Anja Eggers for the construction of oxygen microsensors. We thank Brad Bebout, Volker Meyer and Einar Larsen for developing the data acquisition software and hardware that were used in this study. We gratefully acknowledge the fruitful discussions with Ferran Garcia-Pichel and Olivier Pringault. Olivier Pringault is thanked for his comments and improvements on an earlier version of the manuscript. Part of this study was supported by the Red-Sea Research Programme, Project E 'Microbial activities in hypersaline interfaces controlling nutrient fluxes', financed by the German Ministry for Research and Development (BMBF).

References

Abdollahi, H., and Nedwell, D.B. (1979) Seasonal temperature as a factor influencing bacterial sulfate reduction in a saltmarsh sediment. *Microb Ecol* **5**: 73–79.

Bateson, M.M., and Ward, D.M. (1988) Photoexcretion and fate of glycolate in a hot spring cyanobacterial mat. *Appl Environ Microbiol* **54**: 1738–1743.

Bauld, J., and Brock, T.D. (1974) Algal excretion and bacterial assimilation in hot spring algal mats. *J Phycol* **10**: 101–106.

Berry, J.A., and Raison, J.K. (1981) Responses of macrophytes to temperature. In *Physiological Plant Ecology, I Response to the Physical Environment*, **Vol. 12a**. Lange, O.L., Nobel, P.S., Osmond C.B., and Ziegler, H. (eds). Berlin: Springer Verlag, pp. 277–338.

Blanchard, G.F., Guarini, J.-M., Richard, P., Gros, Ph., and Mornet, F. (1996) Quantifying the short-term temperature effect on light-saturated photosynthesis of intertidal microphytobenthos. *Mar Ecol Prog Ser* **134**: 309–313.

Broecker, W.S., and Peng, T.H. (1974) Gas exchange rates between air and sea. *Tellus* **26**: 21–35.

Cadée, G.C., and Hegeman, J. (1977) Distribution of primary production of the benthic microflora and accumulation of organic matter on a tidal flat area, Balgzand, Dutch Wadden Sea. *Neth J Sea Res* **11**: 24–41.

Canfield, D.E., and Des Marais, D.J. (1993) Biogeochemical cycles of carbon, sulfur, and free oxygen in a microbial mat. *Geochim Cosmochim Acta* **57**: 3971–3984.

Castenholz, R.W. (1976) The effect of sulfide on the bluegreen algae of hot springs. I. New Zealand and Iceland. *J Phycol* **12**: 54–68.

Cohen, Y., Jørgensen, B.B., Revsbech, N.P., and Poplawski, R. (1986) Adaptation to hydrogen sulfide of oxygenic and anoxygenic photosynthesis among cyanobacteria. *Appl Environ Microbiol* **51**: 398–407.

Colijn, F., and Van Buurt, G. (1975) Influence of light and temperature on the photosynthetic rate of marine benthic diatoms. *Mar Biol* **31**: 209–214.

Davison, I.R. (1991) Environmental effects on algal photosynthesis: temperature. *J Phycol* **27**: 2–8.

De Wit, R., Van Boekel, W.H.M., and Van Gemerden, H. (1988) Growth of the cyanobacterium *Microcoleus chthonoplastes* on sulfide. *FEMS Microbiol Ecol* **53**: 203–209.

Epping, E.H.G., Khalili, A., and Thar, R. (1999) Photosynthesis and the dynamics of oxygen consumption in a microbial mat as calculated from transient oxygen microprofiles. *Limnol Oceanogr* **44**: 1936–1948.

Fründ, C., and Cohen, Y. (1992) Diurnal cycles of sulfate reduction under oxic conditions in cyanobacterial mats. *Appl Environ Microbiol* **58**: 70–77.

Garlick, S., Oren, A., and Padan, E. (1977) Occurrence of facultative anoxygenic photosynthesis among filamentous and unicellular cyanobacteria. *J Bacteriol* **129**: 623–629.

Glud, R.N., Jensen, K., and Revsbech, N.P. (1995) Diffusivity in

surficial sediments and benthic mats determined by use of a combined N_2O – O_2 microsensor. *Geochim Cosmochim Acta* **59**: 231–237.

Grant, J. (1986) Sensitivity of benthic community respiration and primary production to changes in temperature and light. *Mar Biol* **90**: 299–306.

Guasch, H., and Sabater, S. (1995) Seasonal variations in photosynthesis-irradiance responses by biofilms in mediterranean streams. *J Phycol* **31**: 727–735.

Guerrero, R., Urmeneta, J., and Rampone, G. (1993) Distribution of types of microbial mats at the Ebro Delta, Spain. *Biosystems* **31**: 135–144.

Hill, W.R., and Boston, H.L. (1991) Community development alters photosynthesis-irradiance relations in stream periphyton. *Limnol Oceanogr* **36**: 1375–1389.

Iversen, N., and Jørgensen, B.B. (1993) Diffusion coefficients of sulfate and methane in marine sediments: Influence of porosity. *Geochim Cosmochim Acta* **57**: 571–578.

Jassby, A.D., and Platt, T. (1976) Mathematical formulation of the relationship between photosynthesis and light for phytoplankton. *Limnol Oceanogr* **21**: 540–547.

Jørgensen, B.B., and Revsbech, N.P. (1985) Diffusive boundary layers and the oxygen uptake of sediments and detritus. *Limnol Oceanogr* **30**: 111–122.

Jørgensen, B.B., Cohen, Y., and Revsbech, N.P. (1986) Transition from anoxygenic to oxygenic photosynthesis in a *Microcoleus chthonoplastes* cyanobacterial mat. *Appl Environ Microbiol* **51**: 408–417.

Kühl, M., Glud, R.N., Ploug, H., and Ramsing, N.B. (1996) Microenvironmental control of photosynthesis and photosynthesis-coupled respiration in an epilithic cyanobacterial biofilm. *J Phycol* **32**: 799–812.

Kühl, M., Lassen, C., and Revsbech, N.P. (1997) A simple light meter for measurements of PAR (400–700 nm) with fiber-optic microprobes: application for P vs. E_0 (PAR) measurements in a microbial mat. *Aq Microb Ecol* **13**: 197–207.

Li, Y.H., and Gregory, S. (1974) Diffusion of ions in sea water and in deep-sea sediments. *Geochim Cosmochim Acta* **38**: 703–714.

Li, W.K.W., Smith, J.C., and Platt, T. (1984) Temperature response of photosynthetic capacity and carboxylase activity in Arctic marine phytoplankton. *Mar Ecol Prog Ser* **17**: 237–243.

Lorenzen, J., Glud, R.N., and Revsbech, N.P. (1995) Impact of microsensor caused changes in diffusive boundary layer thickness on O_2 profiles and photosynthetic rates in benthic communities of microorganisms. *Mar Ecol Prog Ser* **119**: 237–241.

Mir, J., Martínez-Alonso, M., Esteve, I., and Guerrero, R. (1991) Vertical stratification and microbial assemblage of a microbial mat in the Ebro Delta (Spain). *FEMS Microbiol Ecol* **86**: 59–68.

Moezelaar, R., and Stal, L.J. (1994) Anaerobic dark energy generation in the mat-building cyanobacterium *Microcoleus chthonoplastes*. In *Microbial Mats Structure, Development and Environmental Significance*, **Vol. 35**. Stal, L.J., and Caumette, P. (eds). Berlin: Springer Verlag, pp. 273–278.

Nelson, D.C., Revsbech, N.P., and Jørgensen, B.B. (1986) Microoxic-anoxic niche of *Beggiatoa* spp. Microelectrode survey of marine and freshwater strains. *Appl Environ Microbiol* **52**: 161–168.

Padan, E. (1979) Impact of facultatively anaerobic phototrophic metabolism on ecology of cyanobacteria (blue-green algae). In *Advances in Microbial Ecology, Vol 3.* Alexander, M. (ed.). New York: Plenum Press, pp. 1–48.

Pamatmat, M.M. (1997) Non-photosynthetic oxygen production and non-respiratory oxygen uptake in the dark: a theory of oxygen dynamics in plankton communities. *Mar Biol* **129**: 735–746.

Pinckney, J., and Zingmark, R.G. (1993) Photophysiological responses of intertidal benthic microalgal communities to in situ light environments: methodological considerations. *Limnol Oceanogr* **38**: 1373–1383.

Pomeroy, L.R. (1959) Algal productivity in saltmarshes of Georgia. *Limnol Oceanogr* **4**: 386–397.

Rasmussen, M.B., Henriksen, K., and Jensen, A. (1983) Possible causes of temporal fluctuations in primary production of the microphytobenthos in the Danish Wadden Sea. *Mar Biol* **73**: 109–114.

Revsbech, N.P. (1989) An oxygen microelectrode with a guard cathode. *Limnol Oceanogr* **34**: 474–478.

Revsbech, N.P., and Jørgensen, B.B. (1983) Photosynthesis of benthic microflora measured with high spatial resolution by the oxygen microprofile method: capabilities and limitations of the method. *Limnol Oceanogr* **28**: 749–756.

Rivkin, R.B. (1990) Photoadaptation in marine phytoplankton: variations in ribulose-1,5-bisphosphate activity. *Mar Ecol Prog Ser* **62**: 61–72.

Sukenik, A., Bennett, J., and Falkowski, P. (1987) Light-saturated photosynthesis limitation by electron transport or carbon fixation? *Biochim Biophys Acta* **891**: 205–215.

Thamdrup, B., Hansen, J.W., and Jørgensen, B.B. (1998) Temperature dependence of aerobic respiration in a coastal sediment. *FEMS Microbiol Ecol* **25**: 189–200.

Vosjan, J.H. (1974) Sulphate in water and sediment of the Dutch Wadden Sea. *Neth J Sea Res* **8**: 208–213.

Wieland, A., and Kühl, M. (2000) Short-term temperature effects on oxygen and sulfide cycling in a hypersaline cyanobacterial mat (Solar Lake, Egypt). *Mar Ecol Prog Ser* **196**: 87–102.